INFLUENCE OF ULTRASONIC SPATIAL WAVES OVER EFFICIENCY IMPROVEMENT TO WEDM PROCESS

Viorel-Mihai NANI[1,2]

[1] University Politehnica Timisoara, Research Institute for Renewable Energy, G. Muzicescu Street, no. 138, Timisoara, Romania 300774, viorel.nani@upt.ro

[2] University ″Ioan Slavici″ Timisoara, Faculty of Engineering, Paunescu Podeanu Street, no. 144, Timisoara, 300568 Romania, viorelnani@yahoo.com

ABSTRACT: The paper presents results of experimental research for the processing efficiency improvement of the Wire-Cut Electrical Discharge Machines. These machines use a wire like an electrode and are abbreviated WEDM. The WEDM machines were equipped with special devices for the simultaneous ultrasonic activation of the wire electrode in two points after two rectangular directions in space. It was noticed that the ultrasound energy which was introduced in the working environment, influenced the performance parameters of the machining process. The erosion capacity variation, accuracy, shape deviation and roughness for different materials, depending on how were prescribed the technological parameters (the intensity for dielectric breakdown and the ultrasound generators power), is presented under graphic and tabular form.

KEY WORDS: WEDM processing; wire electrode ultrasonic activation; erosive capacity; shape deviation; surface roughness; spatial waves

1. INTRODUCTION

Seventy years after Lazarenko first proposed electrical discharge machining (EDM), the technique has become one of the most commonly utilized unconventional processing technologies. The process of a single electrical discharge involves several phases [1, 2]: dielectric breakdown, plasma and bubble formation, workpiece melting and vaporization, plasma and bubble extension, plasma collapse and removal material. During EDM process, material is removed by means of a series of high-frequency, repeated electrical discharges between the workpiece and tool-electrode [3-6]. Thus, the processing by EDM is a method of machining, based on the destruction and eviction of the material from the workpiece surface, through the dynamic repetitive action of some erosion agents. These agents can have as a form solid, liquid or gaseous particles, plasma, or electromagnetic radiation [5, 7].

The EDM highlight a wide range of physical, chemical (or a combination of those) phenomena, such as abrasive, thermal, chemical and electrical erosion, which are finally leading to the material removal [8-11]. The electrodischarge processing technologies are conditioned by the following factors [2]: 1) the technological equipment structure; 2) the effect energy; 3) the machine command subsystem.

On the other hand, the Wire Electrical Discharge Machining (W-EDM), is a manufacturing process whereby a desired shape is obtained using electrical discharges (sparks) [11]. Material is removed from the workpiece by a series of rapidly recurring current discharges between two electrodes (in the gap), separated by a dielectric liquid (deionized water) and subject to an electric voltage. One of the electrodes is called the tool-electrode, or *wire electrode*, while the other is called the workpiece-electrode, or *workpiece*. The wire electrode connects to a pole and workpiece connects to the other pole of a voltage pulse generator. The process depends upon the fact that the wire electrode and the workpiece are not making actual physical contact [12].

Evacuation of the erosion products from the gap, and restoring the optimum disruptive distance with the help of the wire electrode feeding, ensures the macroscopic continuity of the machining process. Spatial displacement of the electric discharges, accompanied by a geometric modification of the gap, leads to the generation of a desired surface on the workpiece. Dosage of impulse energy has as immediate effect the individualization of the erosion elementary acts, characterising the totality of phenomena that occur during a singular W-EDM pulse. Main processes taking place in the gap during an elementary act of erosion are [4, 13 and 14]: 1) the priming of the electrical discharge; 2) the evolution of the electrical discharge; 3) the material removal from electrodes.

The control and maintaining constant the energy corresponding for each electrical discharge ensures high technological performances that are characterizing W-EDM processing. *Speed of erosion process* or *erosive capacity* $\bar{C}_e$, which is specific to

W-EDM processing, is a multivariable function by form [2, 8 and 15]:

$$\bar{C}_e = f(k_m, h, d, g, \rho_i, U_0, v_e) \quad (1)$$

where: k_m – a constant which takes into account the electrodes material and nature of dielectric liquid; h – workpiece thickness; d – wire electrode diameter; g – gap; ρ_i – resistivity/conductivity of the dielectric liquid; U_0 – idle voltage; v_e – feed speed (displacement speed of wire electrode on machining direction)

Among the parameters that significantly influence the erosion capacity $\bar{C}_e$ and are the most disrupted during the erosive act, are found to be the gap g and the h workpiece thickness measured in the feed direction. The variation of the feed speed v_e determine the change of the distance between electrodes, and therefore, the erosive capacity $\bar{C}_e$ it changes [16].

To maximize the erosion speed in given technological circumstances, imposed by the machining process, it is requires ensuring a balance between the $\bar{C}_e$ erosion speed and the feed speed v_e for obtain and maintain optimum function [17]:

$$\bar{C}_e = v_e \quad \rightarrow \quad max \quad (2)$$

This function it is ensured by a stable relative position between the wire electrode and workpiece and it is defined through an optimum value of the gap size g_{opt}. Mainly, the systems conception for automatic adjustment of the gap is based on the following observations which were deducted logically or empirically [14]: (1) the gap is controlled not from geometrical point of view, but from physically, so that its size is continuously measured by determining the instantaneous resistivity/conductivity of dielectric liquid used to W-EDM; (2) the optimum value of the gap g_{opt} is a complex factor which is influenced by the multitude of specific parameters to W-EDM process; these parameters it is change continuously, having a random character on throughout the manufacturing process; (3) under the conditions in which occur complex phenomena, that have the effect of removing material from the workpiece surface, the control and maintaining to a preset value of the gap, it needed the use a flexible mechanical system that to allow the feed speed variation of the wire electrode around an optimum value.

2. LITERATURE REVIEW

The electrodischarge processing with ultrasonic wire electrode activated is one highly complex technological process. The concept of a viable mechanism for the electrodischarge processing in ultrasonic field it based on logical interconnection of some known phenomena, experimented and applied by various researchers, resulting into overlapping effects and adjacent processes. Ikeda [18] wrote the first report on the bubble's motion in gap during a single electrical discharge, and Mironoff [4] studied the thermal effects of erosive pulses. Okada A. et al [11] have evaluated the sparks distribution and wire vibration in W-EDM using a high-speed camera observation. Recently, Kitamura T. and Kunieda M. [10] clarified the EDM gap phenomena using transparent electrodes. On the other hand, Mitkevici [15] and Murti V.S.R. and Philip P.K [19], showed that for maintaining the erosion capacity to an approximately constant value during the machining process, it is requires a further wash under hydrostatic pressure of the gap and the wire electrode vibration.

The first experiments regarding the massive electrodes vibration were undertaken by Mitkevici [15]; in the same time, Inoue [20] has patented the first devices for ultrasonic activation of the wire electrode. One such ultrasonic activation device of the wire electrode used on the W-EDM machines is shown schematically in Figure 1.

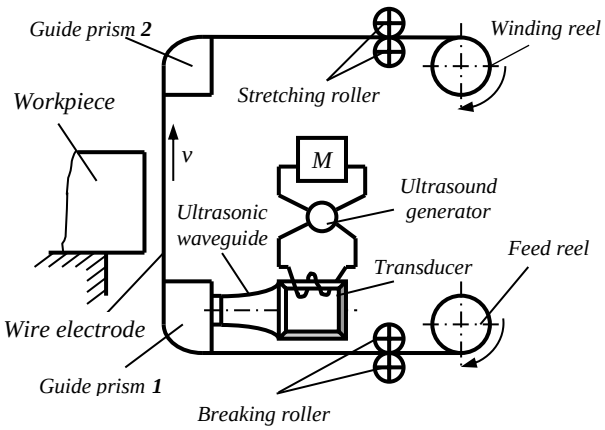

Fig. 1 An ultrasonic activation device of the wire electrode provided with a frequency modulator
M – frequency modulator; *v* – movement speed of the wire electrode along its axis

The ultrasonic activation device is provided with a modulator *M* that modifies controlled timed the signal frequency provided by the ultrasound generator. In this way it changes the number of nodes and antinodes into the wire electrode between guide prisms ***1*** and ***2***, resulting a constant displacement of their positions along the wire electrode. This results in a uniformly processed front surface in workpiece. However, the use of this device is limited by the frequency range in transducer can be activated, for as together with the ultrasonic waveguide to be work at the resonance frequency. For this reason, are using transducers by magnetostrictive type.

Another type of device patented by Inoue [20] is shown schematically in Figure 2. This one consists a complex guiding element, fixed into a support which is able to oscillates after two rectangular directions in the horizontal plane due to transducers ***1*** and ***2***.

Each transducer is independently activated from an

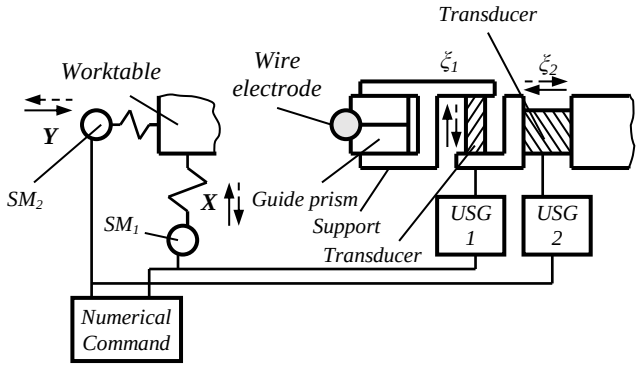

Fig. 2 An ultrasonic activation device of the wire electrode provided with a support which can oscillate after two rectangular directions in horizontal plane

$USG_{1,2}$ – independent ultrasonic generators ***1*** and ***2***; *$SM_{1,2}$* – stepper motor for entraining the worktable ***1*** and ***2***; *X, Y* – displacement directions of the working table in horizontally plane; *ξ_1, ξ_2* - the vibration amplitude of the transducers ***1*** and ***2***

ultrasonic generator *$USG_{1,2}$*, which are controlled by one numerical command. The numerical command controls the worktable movements after directions ***X-Y*** by acting of the stepper motors *$SM_{1,2}$* depending on the workpiece geometric configuration. Since the dimensional accuracy of the W-EDM with ultrasonic activated wire electrode is affected by non-concordance between the wire vibration direction and the feeding direction, the device ensures successively or simultaneously the vibration of the guide prism.

For increasing the processing accuracy, another device model made by Inoue [20] which is shown in Figure 3, has in its construction a control unit *CU*. On the one hand, it check and adapts continuously the frequency/power ultrasonic generator *USG*, and on the other hand it is electrically connected to a potentiometer *P* disposed between the wire electrode and workpiece. Depending on the arc drop between electrodes (indicated by *P*), the control unit *CU* regulates the frequency and/or amplitude supplied

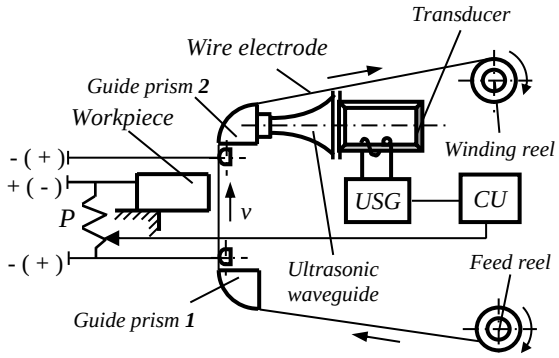

Fig. 3 An ultrasonic activation device of the wire electrode provided with a control unit

USG – ultrasonic generator; *CU* – control unit; *P*– potentiometer;
v – movement speed of the wire electrode along its axis

by *USG* in the wire electrode as to creates optimal conditions of the priming electrical discharges in pulse.

The shortcomings of devices shown above are largely diminished when the wire electrode is simultaneous ultrasonic activated in two points disposed after two rectangular directions in space. Such a device was patented by Savii Gh. et al [21] and is shown schematically in Figure 4. This device was used for conducted all researches in the paper.

The wire electrode receives an oscillatory movement through guide prism ***1*** from an electroacoustic converter (not shown in figure). This one is

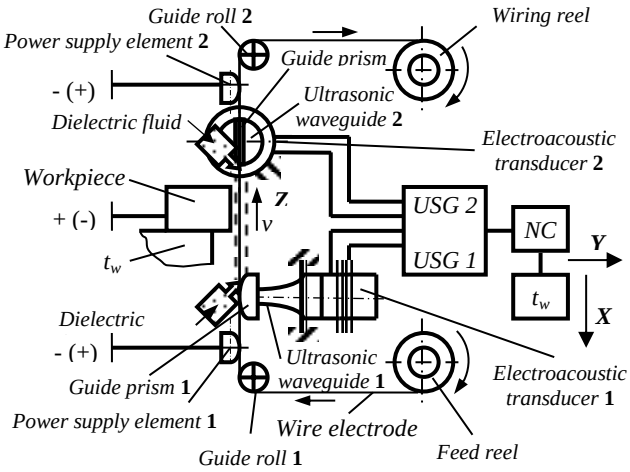

Fig. 4 An ultrasonic activation device of the wire electrode in two points after two rectangular directions in space

$USG_{1,2}$ – ultrasonic generators ***1*** and ***2***; *NC* – numerical command; *t_w*– worktable; v – movement speed of the wire electrode along its axis; *X, Y, Z* – displacement directions of the worktable and *Mobile Arm*

composed from the ensemble formed from the ultrasonic waveguide ***1*** – electroacoustic transducer ***1*** - ultrasound generator *(USG_1)*, and is activated with a certain amplitude and frequency of vibration. Concomitantly, the wire electrode receives another oscillatory movement through the guide prism ***2*** from another electroacoustic converter (not shown in figure). This one is composed from an ultrasonic waveguide ***2*** – electroacoustic transducer ***2***- ultrasonic generator *(USG_2)*, and is activated with an amplitude and frequency of vibration equal to or different from the first. The two vibration directions are perpendicular in space.

Acoustic parameters of the generators *$USG_{1,2}$* are constantly analyzed by the numerical command *NC* and are correlated with the working conditions from the gap through the appropriate command given to the feeding mechanisms after the directions ***X*** and ***Y***. The wire electrode is moving along its axis after the ***Z*** direction which is perpendicular to the ***XY*** reference plane, materialized by the surface of worktable *t_w*; the three directions of movement, ***X***, ***Y*** and ***Z*** are established in conventional way and are

reported to the kinematics of the processing technological equipment.

Theoretical studies were very well thorough either only in electrodischarge processing, either in ultrasound processing. But they could not outline a mechanism that explain in a clear and coherent mode, the elementary processes occurring in the dielectric liquid from the gap. Here occur the energy interference phenomena of the electrical discharges in pulse with the ultrasonic energy. For this reason, it could not be studied in depth the influence of some specific factors for the high energy ultrasounds, like: the ultrasonic activation ways of wire electrode, the composing and the waves interference in wire electrode.

With all complexity of the phenomena involved in machining process, it is assumed that the material removal is influenced by several forces (thermal, mechanical, hydraulics, electrostatic, magnetic, aerodynamics etc.), having different percentages in time. Mironoff [4] highlighted the importance of the thermal effect for removal the material. Chen Z. et al [22] considered the spatial temperature field and the electromagnetic field very important in W-EDM; Hayakawa S. et al [23] showed the effects of bubbles expansion in the electrical discharge machining (hydraulic effect), Cetin S. et al [24] developed the debris accumulation effect due to the machining speed at EDM (electrostatic effect and aerodynamic) etc.

3. TESTING PLANT

The testing plant consists of a W-EDM machine, ELEROFIL-10 type, made by SC STIMEL SA [25]. The ultrasonic activation of the wire electrode is performed with the help of two special devices, invented by Savii Gh. et al [21]. These are mounted into the wire electrode drive mechanism structure, in close proximity of working area. Through them, we targeted improving efficiency of W-EDM machines. Schematic drawing of the testing plant - which it is presented in Nani [16] -, is shown in Figure 5.

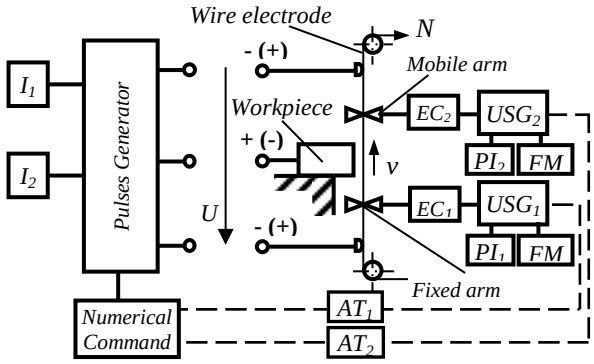

Fig. 5 General principle scheme of the testing plant

$I_{1,2}$ – electrical current intensity for breakdown dielectric liquid; adjustable parameter in two steps, gross I_1 and fine $I_{2;}$ U_i – priming voltage of electrical discharges corresponding to intensity parameter *I; v* - movement speed of the wire electrode along its axis; *N* – stretching force of the wire electrode; $EC_{1,2}$ – electroacoustic converter 1 and 2 corresponding to f*ixed* or *mobile arm;* $USG_{1,2}$ – ultrasonic generator corresponding to $EC_{1,2}$; $PI_{1,2}$ – power indicator for $USG_{1,2}$; $FM_{1,2}$ - frequency monitor; $AT_{1,2}$ - autotransformer 1 and 2

We conventionally denoted by USG_1 the ultrasonic generator which transmits a high frequency signal toward the EC_1 electroacoustic converter mounted in the fixed arm; respectively with USG_2 the ultrasonic generator assembled with EC_2 in the mobile arm. The $EC_{1,2}$ electroacoustic converter is a mechanical assembly that comprises a piezoceramic transducer, an ultrasonic waveguide 1 and 2, and two guide prisms of the wire electrode made from sapphire or diamond.

The power supply element of the each ultrasonic generator is composed mainly from one autotransformer $AT_{1,\ 2}$ and one power indicator $PI_{1,2}$. The vibration frequency supplied by each ultrasonic generator is measured continuously during the machining process with the help of a frequency monitor by $FM_{1,\ 2}$.

A design constructive solution of the drive mechanism of the wire electrode is shown in Figure 6. This mechanism allows the displacement of wire electrode after two directions ***Y*** and ***Z***, and workpiece together with worktable are moving after the ***X*** direction [25]. The directions ***X***, ***Y*** and ***Z*** are set in a conventional manner in relation with the kinematic structure of the W-EDM machine. The drive mechanism of the wire electrode is further provided with a subassembly composed from braking roll - drive roll 2 located immediately after the feed reel, and another subassembly composed from stretching roll – drive roll 1, where the stretching roll has the size lower than braking roll. Through synchronization and control of relative movement of rotation between the braking roll and stretching roll, is ensures greater stability to the movement of wire electrode between guide prisms 1 and 2, so that the speed of the wire electrode in the direction Z is controlled by the braking roll, and the tensile force in wire electrode depends on the angular velocity of stretching roll.

The workpiece is installed and fixed onto the worktable of the W-EDM machine and is moving in

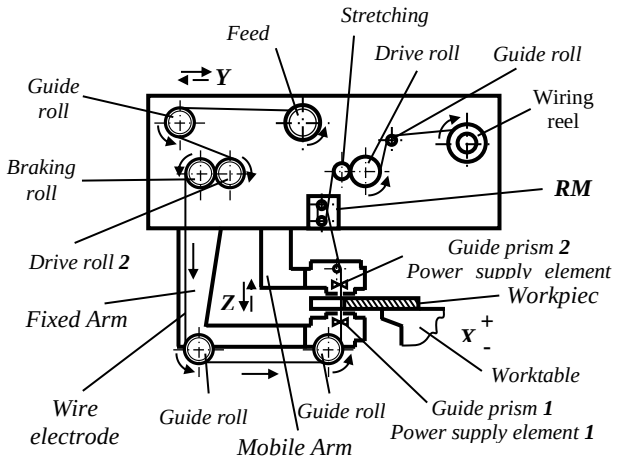

Fig. 6 Scheme of the wire electrode drive mechanism of the ELEROFIL-10 machine

RM –regulator mechanism; *X, Y, Z* – displacement directions of the *worktable* and *drive mechanism* in horizontally, respectively in vertical plane for *Mobile Arm*

the ***X*** direction (see Figure 7). In turn, ultrasonic waveguides 1 and 2 are stiffened onto the fixed arm, respectively mobile arm, and are moving in the ***Y*** direction together with the wire electrode drive mechanism.

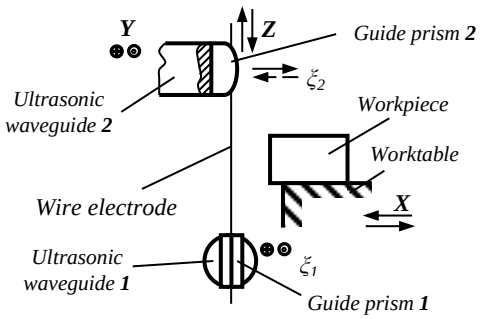

Fig.7 Kinematic scheme of machine and the ultrasonic activation devices
$\xi_{1,2}$ – vibration amplitude in the mobile or fixed arm; *X, Y, Z* – displacement directions conventional established

The wire electrode is moving along its axis after the ***Z*** direction, which is perpendicular to the ***XY*** reference plane materialized by the worktable surface; the three directions of movement ***X***, ***Y*** and ***Z*** are established conventionally and are reported to the kinematics of the processing equipment.

The subassembly ultrasonic waveguide – guide prism 1 is disposed in space perpendicular compared to ultrasonic waveguide – guide prism 2 such that guide prism 1 vibrates after direction ***Y*** with vibration amplitude ξ_1, simultaneously with the guide prism 2 which vibrating after direction ***X*** with ξ_2 amplitude. Amplitudes of the two movements are perpendicular from each other, and through their combination are obtained *spatial waves* as shown in Nani [17].

The electrical scheme of the wire electrode ultrasonic activation is shown in Fig. 8.

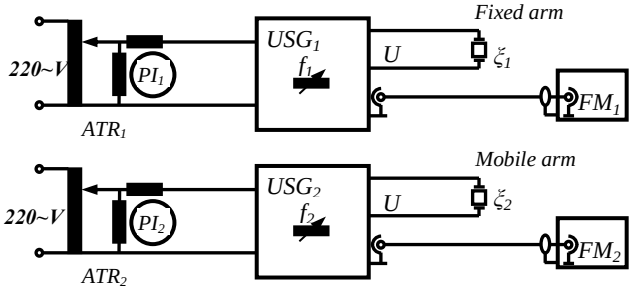

Fig. 8 The electrical scheme for the wire electrode ultrasonic activation in two points after two rectangular directions in space
$AT_{1,2}$ – autotransformer 1 and 2; $USG_{1,2}$ – ultrasonic generators 1 and 2; *US* – a high-frequency (ultrasound); $PI_{1,2}$ – power indicator for $USG_{1,2}$; $FM_{1,2}$ - frequency monitor; $f_{1,2}$ – frequencies provided by ultrasonic generator 1 and 2; $\xi_{1,2}$ – vibration amplitude in fixed arm 1, respectively in mobile arm 2

By continuously altering the autotransformer $AT_{1,2}$, supply voltage of the ultrasonic generator $USG_{1,2}$ the activation power it is changes. In this way we can obtained a variable acoustic power which determines the variation of vibrational amplitude $\xi_{1,2}$ of one of the guiding elements GE_1 or GE_2. The guiding elements are those that finally transmit the vibrational movement with ultrasonic frequency at the wire electrode.

Any ultrasound generator, by its constructive solution, allows auto-adjustment to the resonance frequency during machining process. USG1,2 ensures the maximum acoustic power transfer even to the relatively large variations of the mechanical impedance, as confirmed by the frequency monitor.

4. ULTRASONIC ACTIVATION PRINCIPLE OF THE WIRE ELECTRODE

The scheme for the simultaneous ultrasonic activation of the wire electrode in two points after two perpendicular directions in space used at the W-EDM machining was developed in Nani [26]. An example is illustrated in Figure 9.

Into point ***2***, the wire electrode is ultrasonic activated after a direction with the vibrational amplitude and frequency denoted with $\xi_{WE}^{(2)}$, $f_{WE}^{(2)}$. Into point **3** located at a distance l_i compared to the point **2**, the wire electrode is ultrasonic activated with a vibrational amplitude and frequency denoted with $\xi_{WE}^{(3)}$, $f_{WE}^{(3)}$, after a perpendicular direction in space toward first direction. In the event that the vibration amplitudes $\xi_{WE}^{(2)}$ and $\xi_{WE}^{(3)}$ it varies harmonic, in accordance with Yamada et al [27], the wire electrode achieves two *orthogonal harmonic oscillations*. From the point of view of practical applications, it is interesting to determine the trajectory and the composed vibration amplitude into the wire electrode. The distance l_i between guide prisms **1** and **2** is variable and can be adjusted according to the workpiece thickness. In the scheme shown in Figure 9 it is considered that l_i is constant. Also, the distances l_i' and l_i'' are constant and are defined based on construction and functionability.

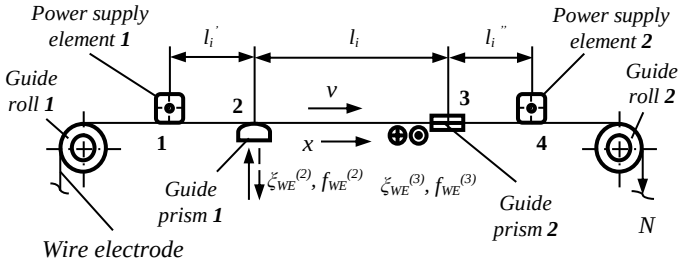

Fig. 9 The principle scheme for ultrasonic activation of the wire electrode in two points after two rectangular directions in space
$\xi_{WE}^{(2)}$, $f_{WE}^{(2)}$ – amplitude and vibrational frequency of the wire electrode in the point **2**; $\xi_{WE}^{(3)}$, $f_{WE}^{(3)}$ - amplitude and vibrational frequency of the wire electrode in the point **3**; l_i, l_i', l_i'' - lengths between the guiding and power elements; *N* – stretching force of the wire electrode; *v* – movement speed of the wire electrode along its axis; **1**, **2**, **3** and **4** - points of contact of the wire electrode with the power elements and the guiding elements; *x* - direction of wave movement

4.1 When the two orthogonal harmonic vibrations have same frequency

If the two orthogonal harmonic vibrations have the same frequency $f^{(2)} = f^{(3)} = f$, then the motion law of the wire electrode for own mode of vibration n it can be written as follows:

$$\xi_n^{(2)}(x,t) = (A_n \cos k_n t + B_n \sin k_n t) \sin k_n x \qquad (3.a)$$

$$\xi_n^{(3)}(x,t) = [A_n \cos(k_n t + \varphi_n) + B_n \sin(k_n t + \varphi_n)] \sin(k_n x + \varphi_n) \qquad (3.b)$$

Depending on the φ_n difference in phase, the trajectory of the wire electrode in a plane normal to *0x* direction for advance (along its axis), it can occupy an infinite number of positions. For some particular values of the φ_n difference in phase, the trajectory of the wire electrode in a perpendicular plane to its displacement direction is shown in the diagrams from Figure 10.

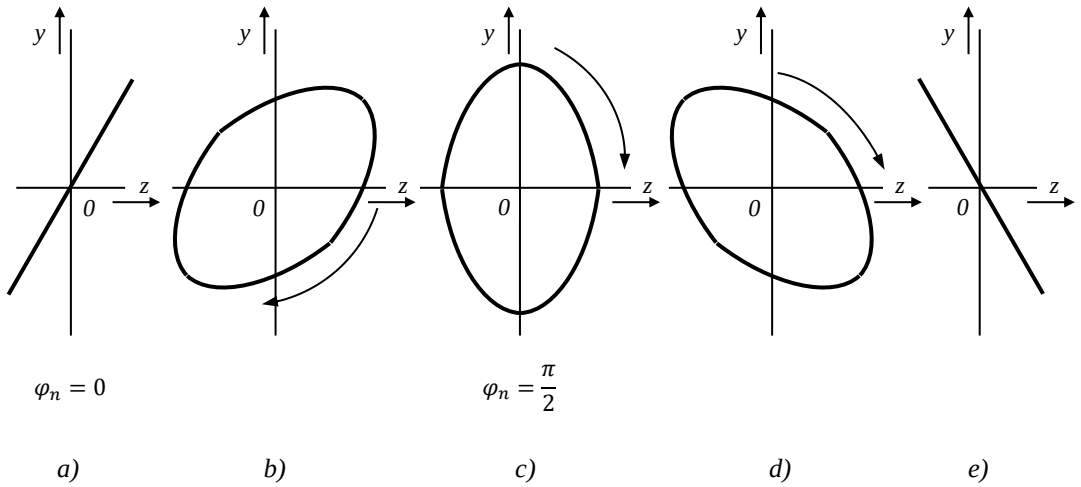

Figure 10 The trajectory of the wire electrode in a plane normal to its displacement direction (along its axis) according to the difference in phase

y0z - system of rectangular axes in a plane normal to the wire electrode displacement direction

When the difference in phase is $\varphi_n = 0$, then the trajectory of the wire electrode is a straight line contained in quadrants *I* and *III* of the system by Cartesian coordinate *y0z* (see Figure 10.a), and the vibration amplitudes are found in the ratio:

$$\frac{\xi_n^{(2)}}{\xi_{WE}^{(2)}} = \frac{\xi_n^{(3)}}{\xi_{WE}^{(3)}} \qquad (4)$$

If the two vibration amplitudes movements are equal:

$$\xi_{WE}^{(2)} = \xi_{WE}^{(3)},$$

then for $\varphi_n = 0$, the trajectory of the wire electrode is a straight line contained in quadrants *I* and *III* and it is located at 45^0. Similarly, when the difference in phase is $\varphi_n = \pi$, the wire electrode describes a segment symmetrically toward origin on a straight line contained in quadrants *II* and *IV* of the system by Cartesian coordinates *y0z* (see Figure 10.e), and the vibration amplitudes are found in the ratio:

$$\frac{\xi_n^{(2)}}{\xi_{WE}^{(2)}} = -\frac{\xi_n^{(3)}}{\xi_{WE}^{(3)}} \qquad (5)$$

For other values of the φ_n difference in phase, by eliminating the $k_n t$ argument from equations system (3.a and 3.b), it obtained the equation that defines the trajectory of the wire electrode:

$$\frac{{\xi_n^{(2)}}^2}{{\xi_{WE}^{(2)}}^2 \sin^2\varphi_n} + \frac{{\xi_n^{(3)}}^2}{{\xi_{WE}^{(3)}}^2 \sin^2\varphi_n} - \frac{2\,\xi_n^{(2)}\xi_n^{(3)} \cos\varphi_n}{\xi_{WE}^{(2)}\xi_{WE}^{(3)} \sin^2\varphi_n} = 1 \qquad (6)$$

It can be noted that the trajectory of the wire electrode in the y0z plane is an ellipse with center in origin. The ellipses axes are inclined compared to axes the Cartesian coordinate system (see Figure10.b and 10.d). In the particular case, for $\varphi_n = \frac{\pi}{2}$, the axes of ellipses coincide to the axes of the coordinate system *y0z*. For these situations, the ellipse equation is:

$$\frac{{\xi_n^{(2)}}^2}{{\xi_{WE}^{(2)}}^2} + \frac{{\xi_n^{(3)}}^2}{{\xi_{WE}^{(3)}}^2} = 1 \qquad (7)$$

If the vibration amplitudes are equal

$$\xi_{WE}^{(2)} = \xi_{WE}^{(3)},$$

the trajectory of the wire electrode in the *y0z* plane is *a circle*. This finding is particularly important for the W-EDM machining with ultrasonic activated wire electrode in two points after two rectangular directions in space, directly influencing the shape and dimensional accuracy of the workpiece.

The trajectory of the wire electrode is also distorted in the *y0x* plane, according to the difference in phase between the two movements. In Figure 11 are illustrated few particular cases for distortion of the

trajectory of the wire electrode in a plane containing its displacement direction along its axis.

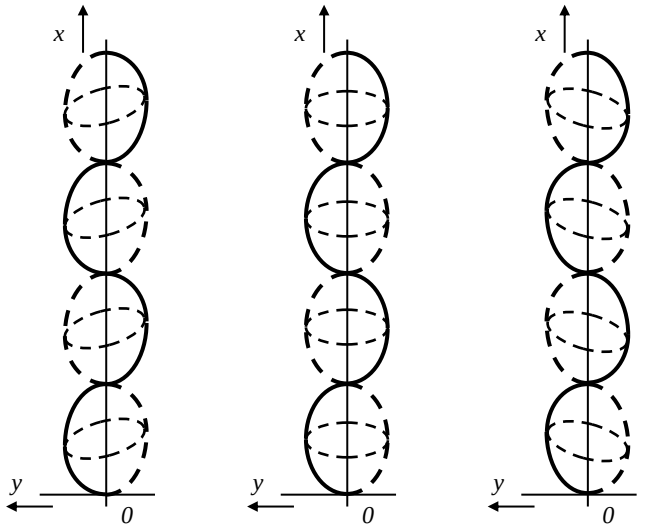

Figure 11 The trajectory of the wire electrode in a plane parallel to its displacement direction according to the difference in phase
x0y - system of rectangular axes in a plane parallel to the wire electrode displacement direction

When the difference in phase between the two movements is $\varphi_n = \frac{\pi}{4}$ or $\varphi_n = \frac{3\pi}{4}$, then the trajectory of the wire electrode is asymmetric with respect to the *0x* axis (see Figure11.a and 11.c), being slightly elongated *into* or *toward* the displacement sense of the ultrasonic waves. For the case when $\varphi_n = \frac{\pi}{2}$, the trajectory of the wire electrode is symmetric toward the *0x* axis (see Figure 11.b).

The resultant vibrational amplitude is maxim in the particular case $\xi_{WE}^{(2)} = \xi_{WE}^{(3)}$ and is given by

$$\xi_n^{(r)} = \sqrt{2}\,\xi_{WE}^{(2)} \tag{8}$$

For the fundamental mode of vibration *n = 1*, the variation scheme of the wire electrode amplitude between points **1-2**, **2-3** and **3-4** is shown in Figure12.

If between the points **1-2** and **3-4** the vibration of wire occurs after one perpendicularly direction relative to another direction according to the motion laws given by equations (3.a and 3.b), then for practitioner becomes interesting the interference mode of waves into section **2-3**, i.e., the portion which is in connection with the workpiece.

When $\xi_{WE}^{(2)} = \xi_{WE}^{(3)}$, the vectorial scheme for the combination of the orthogonal harmonic movements having same vibrational frequency is shown in Figure 13. For $tan\,\psi = 1$, resulting $\psi = 45^0$.

Vibration amplitude of the wire electrode is maxim for the positions - see relationships (3.a) and (3.b) -:

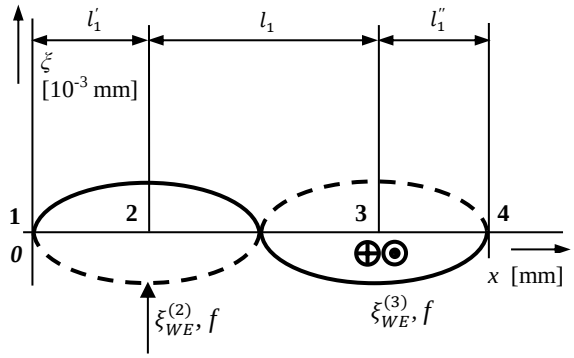

Figure 12 Amplitude's variation diagram of the wire electrode for the vibration mode *n = 1*, corresponding the drawing from Figure 9
ξ – vibration amplitude; $\xi_{WE}^{(2)}, \xi_{WE}^{(3)}$ – vibration amplitudes of the wire electrode in the points **2** and **3**; l_i, l_i', l_i'' - lengths between the guiding and power elements of the wire electrode denoted **1**, **2**, **3** and **4** for vibration mode *n = 1*; *f* – vibration frequency of the wire electrode in the points **2** and **3**; *x* – abscissa; **1**, **2**, **3** and **4** - points of contact for the wire electrode with the guiding and power elements

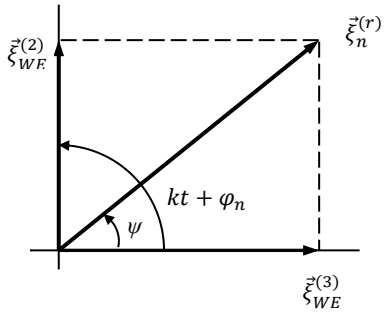

Figure 13 Combination of the orthogonal harmonic movements having the same vibrational frequency
$\vec{\xi}_{WE}^{(2)}, \vec{\xi}_{WE}^{(3)}$ – vectors of the wire electrode vibrational amplitudes in the points **2** and **3**; $\vec{\xi}_n^{(r)}$ - resultant vector of vibrational amplitude for vibration mode *n*; *k* - wave number; *t* – time; φ_n – the difference in phase between the two movements

$$\sin\left(\frac{\omega_n x}{c} + \varphi_1\right) = 1 \tag{9}$$

namely:

$$\frac{\omega_n x}{c} + \varphi_1 = (2q+1)\frac{\pi}{2},$$

where $q = 0, 1, 2, \ldots n-1$ (10)

or:

$$\frac{n\pi x}{c} + \varphi_1 = (2q+1)\frac{\pi}{2} \tag{11}$$

from where:

$$x = \frac{2q+1}{2n}l - \varphi_1 \tag{12}$$

4.2 When the two orthogonal harmonic vibrations have different frequencies

In this case, we have $f^{(2)} \neq f^{(3)}$. Motion law of the wire electrode for own mode of vibration *n* is given by the equation:

$$\xi_n^{(2)}(x,t) = \left(A_n \cos k_n^{(2)} t + B_n \sin k_n^{(2)} t\right) \sin k_n^{(2)} x \quad (13)$$

$$\xi_n^{(3)}(x,t) = \left[A_n \cos\left(k_n^{(3)} t + \varphi_n\right) + B_n \sin\left(k_n^{(3)} t + \varphi_n\right)\right] \sin\left(k_n^{(3)} x + \varphi_n\right) \quad (14)$$

Admitting that $f_n^{(3)} > f_n^{(2)}$ and $k_n^{(3)} - k_n^{(2)} = \Delta k_n$, the vectorial representation of the two movements is illustrated in the diagram of Figure 14.

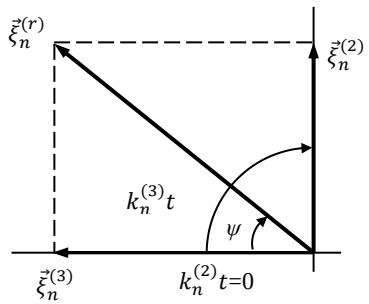

Figure 14 Combination of the orthogonal harmonic movements having different vibration frequencies
$\vec{\xi}_n^{(2)}, \vec{\xi}_n^{(3)}$ – vectors of the wire electrode vibrational amplitudes in the points **2** and **3**; $\vec{\xi}_n^{(r)}$ - resultant vector of vibrational amplitude for vibration mode *n*; $k_n^{(2)}, k_n^{(3)}$ – wave number; *t* – time; φ_n – the difference in phase between the two movements

It is observed that the ψ angle between the vectors $\vec{\xi}_n^{(2)}$ and $\vec{\xi}_n^{(3)}$ is no longer constant. This varies in time and is equal to:

$$\left(k_n^{(3)} - k_n^{(2)}\right) t + \varphi_n = \Delta k_n + \varphi_n \quad (15)$$

For this reason, the resultant vector $\vec{\xi}_n^{(r)}$ which represents the vibration composed of two orthogonal harmonic oscillations but having different frequencies has the size $\left|\vec{\xi}_n^{(r)}\right|$ and difference in phase ψ relative to the first motion. The resultant of vibration amplitude $\left|\vec{\xi}_n^{(r)}\right|$ and difference in phase ψ are variable in time. In this case, resultant size is not harmonic and, generally, nor periodic.

For as the resultant vibratory motion to be periodical, with a period $T^{(r)}$, after Silas et al [28], it needs to be a multiple for both the period:

$$T_n^{(2)} = \frac{1}{f_n^{(2)}} = \frac{2\pi}{\omega_n^{(2)}},$$

as well for the period:

$$T_n^{(3)} = \frac{1}{f_n^{(3)}} = \frac{2\pi}{\omega_n^{(3)}},$$

i.e.:

$$T_n^{(r)} = a_n^{(2)} T_n^{(2)} = a_n^{(3)} T_n^{(3)} \quad (16)$$

where: $a_n^{(2),(3)}$ - integer numbers

For as the resultant $T^{(r)}$ to be minim, it is needs that $a_n^{(2)}$ and $a_n^{(3)}$ to be the coprime numbers:

$$\frac{\omega_n^{(2)}}{\omega_n^{(3)}} = \frac{a_n^{(2)}}{a_n^{(3)}}, \quad (17)$$

namely, the pulsations ratio must be a rational fraction. In these circumstances, the period $T_n^{(r)}$, is and a multiple for the period $T_n^{(r)'}$:

$$T_n^{(r)} = \left(a_n^{(3)} - a_n^{(2)}\right) T_n^{(r)'} \quad (18)$$

If the two pulses have the values very close, the difference $\Delta\omega_n$ is very small. In this case, the periods $T_n^{(r)}$ and $T_n^{(r)'}$ of the component motions are almost equal. During a period $T_n^{(2)}$ and $T_n^{(3)}$, the angle between the representative vectors of component motions varies with (see Figure14):

$$T_n^{(2)} \Delta\omega_n \approx T_n^{(3)} \Delta\omega_n,$$

which is a very small value; for this reason, Silas et al [28] considered that, during a period $T_n^{(2)}$, $T_n^{(3)}$, *the resultant amplitude of vibration motion remains constant*. In this time frame, *the resultant motion can be considered as harmonic*. Within a longer period of time, the resultant motion can be considered as a sequence of harmonic movements, having the same duration or frequency, but with different amplitudes.

The resultant of the vibration amplitude harmonic $\xi_n^{(r)}(x,t)$ varies between the *maximum values:*

$$\sqrt{\xi_{WE}^{(2)^2} + \xi_{WE}^{(3)^2}} \quad (19)$$

when the two vectors have the same sense and *zero value* when the vectors are equals and the opposite sense.

The resultant movements of trajectories of the wire electrode are complex curves, ranging with the ratio:

$$\frac{k_n^{(2)}}{k_n^{(3)}}$$

If this report is a rational number, Yamada et al [27] showed that the curves which define the trajectories of the wire electrode are closed.

5. EXPERIMENTAL INVESTIGATIONS

5.1 Erosion capacity

Experiments have been conducted in same conditions as those were describes in [29] on two types of workpieces. These were made from alloy steel plates *34 MoCrNi 15*, DIN 1.6582, having a thickness of *40* mm and heat treated to *54-56* HRC, as well as from high alloy steel *X210 CRW 12*, DIN

1.2436, having thicknesses of *40* mm and heat treated to *60-62* HRC hardness. Datum surfaces were rectified plane-parallel to ensure a good settlement on the worktable and to allow precise adjustment of wire electrode perpendicular to these surfaces.

The machining technology consisted of cutting slits from one end of some workpieces, all slits having a length of 15 mm. The processing scheme of the workpiece is shown in Figure 15.

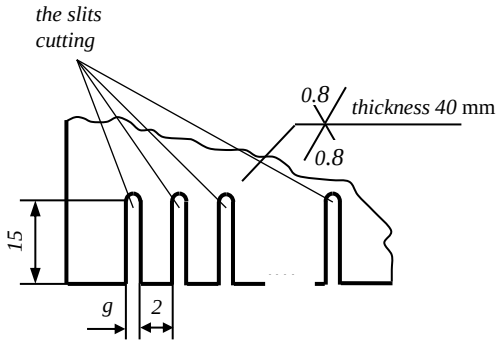

Fig. 15 Workpiece - top view and processing schematics
g – gap (technological interstitium)

Samples in lots of 5 slits cutting were processed. During machining process, were kept constant the following parameters: the movement speed of wire electrode along its axis: *25* mm/s; the stretching force of the wire electrode: *40* N; the absorbed power by ultrasonic generators: *30* W; the resistivity of the dielectric fluid: 10^4 Ω.cm; the ultrasonic activation frequency: *39.900* kHz into fixed arm and *40.160* kHz into mobile arm (the wire electrode was ultrasonically activated simultaneous in two points after two perpendicular directions in space).

As is showed in [16], the erosion capacity was determined as follows:(1) it was programmed the numerical command of the W-EDM machine to perform cuts with the length of 15 mm; when the wire electrode reaches the 15 mm end of cut, the machine stops automatically; (2) the feed speed was controlled by the voltage pulses generator; (3) the vibrational amplitude of the wire electrode was controlled by the ultrasonic generator, by regulating and controlling the electrical power absorbed from the network;

Note: In lab conditions, we measured the vibrational amplitude of the wire electrode using a high speed camera. Thus, we established a correlation between the amplitude of the vibration, the erosive capacity and the power consumption of the ultrasonic generator. Practically, the technologist is not interested in the actual size of the amplitude, but only in the erosion capacity. And this parameter can be controlled easily through the command of W-EDM machine.

(4) the numerical command of the machine W-EDM allowed the actual time measurement of processing; (5) the erosive capacity (erosion speed) was calculated by reporting a prescribed amount (cutting length, which is constant - 15 mm) to a random variable (processing time); (6) in order to evaluate the random errors, the erosive capacity was calculated as the arithmetic mean for five consecutive cuttings in identical technological conditions; similarly, it has been calculated the average value of the gap. Thus, for *L = 15* mm, we have:

$$\bar{C}_e = \frac{1}{5}\sum_{i=1}^{5} C_{ei}\,; \quad C_{ei} = \frac{15\ x\ 60}{t_i}\left[{}^{mm}/_{min}\right]$$

$$\text{and} \qquad \bar{g} = \tfrac{1}{5}\textstyle\sum_{i=1}^{5} g_i \quad [mm] \qquad (20)$$

where t_i is the actual duration of processing (from first to last spark) [sec], and g_i is the actual distance between the edges of the cutting slit [mm].

For samples made of *34 MoCrNi 15*, results are shown in *Table 1*, where US means ultrasound.

Table 1

The variation of erosion capacity and the gap size due to intensity needed for the dielectric fluid breakdown – results obtained with samples made from *34 MoCrNi 15* steel

Parameter	**Processing method**	**Intensity for breakdown dielectric fluid** *I* [A]				
		1.88	2.22	2.90	3.28	4.42
Average erosion capacity $\bar{C}_e$ [mm/min]	Without US activation	*0.401*	*0.424*	*0.465*	*wire electrode often breaks*	-
	With US activation	*0.698*	*0.740*	*0.805*	*0.860*	*0.889*
Average gap size $\bar{g}$ [mm]	Without US activation	*0.455*	*0.458*	*0.447*	-	-
	With US activation	*0.462*	*0.464*	*0.464*	*0.456*	*0.453*

Variation of the average erosion capacity $\bar{C}_e$ and average gap size $\bar{g}$ due to the intensity needed for dielectric fluid breakdown are illustrated in Figure 16.

From the study of diagrams, it is observed an increase in erosion capacity with the increase of the intensity needed for dielectric fluid breakdown, more pronounced when the wire electrode is

ultrasonic activated, with about 73-74% (for same intensity step). Moreover, ultrasonic activation of wire electrode allows adjusting the pulses generator to higher intensities for the electrical current needed for the dielectric breakdown. When processing is

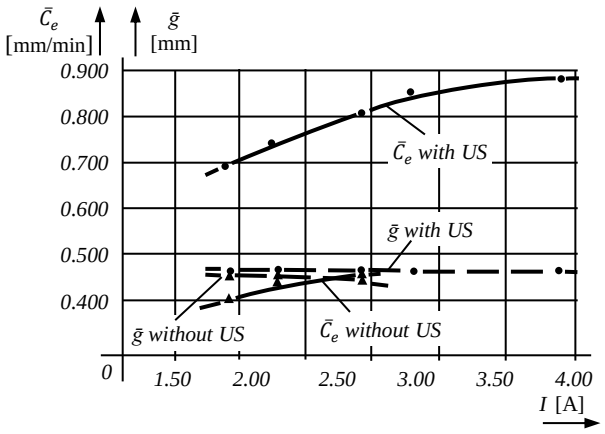

Fig. 16 Average erosive capacity and average gap size due to intensity variation needed for dielectric breakdown - samples made *34 MoCrNi 15* steel

done without ultrasonic activation of the wire electrode, it was found that the wire often breaks when the generator gives current pulses of *3.28* A. For this reason, the machine operator must do wire knotting and continue processing on a lower step by intensity (*2.90* A). On the other hand, the ultrasonic activation of the wire electrode, typically ensures adjustment of the intensity to *4.42* A without disturbances of the technological process. With this, the increase in erosion capacity is about 91-92%.

The gap has sensitively equal values in both cases and remains approximately constant in its variation range of intensity for dielectric breakdown. This observation is important both for the technologist, as well for the programmer in order to define the relative wire electrode position correction compared to the workpiece; this is necessary to ensure a very good dimensional and shape accuracy.

Similarly, for samples made from *X210 CrW 12*, the research results are summarized in *Table 2*. We can notice the fact that the maximum current intensity needed for dielectric fluid breakdown is lower with one step.

Table 2

The variation of erosion capacity and the gap size due to intensity needed for the dielectric fluid breakdown – results obtained on samples made *X210 CrW 12* steel

Parameter	**Processing method**	**Intensity for breakdown dielectric liquid** I [A]				
		1.54	2.56	3.08	3.50	4.22
Average erosion capacity $\bar{C}_e$ [mm/min]	Without US activation	*0.364*	*0.428*	*0.452*	*Wire electrode often breaks*	-
	With US activation	*0.584*	*0.693*	*0.724*	*0.748*	*0.817*
Average gap size $\bar{g}$ [mm]	Without US activation	*0.321*	*0.324*	*0.397*	-	-
	With US activation	*0.324*	*0.324*	*0.356*	*0.357*	*0.365*

Similarly, the average erosion capacity $\bar{C}_e$ and the average gap size $\bar{g}$ due to electrical intensity needed for the breakdown dielectric liquid are illustrated in graphs of Figure 17.

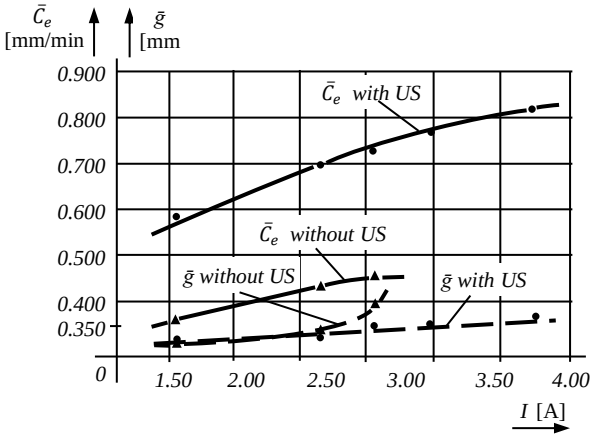

Fig. 17 Average erosive capacity and average gap size due to intensity variation needed for dielectric breakdown - samples made *X210 CrW 12* steel

It is noticed that the scattering of experimental results is higher compared with the material *34 MoCrNi 15*. Generally, the output sizes (erosion capacity and gap) have lower values than in the material processability case *X210 CrW 12*. This is explained by the relatively high content of an alloying element (wolfram), that require higher thermal energies for separation the particles from the crystal lattice and that is more abrasion-proof due to cavitation from the workspace.

Increasing the dielectric liquid breakdown intensity determines the increase of electro-erosive processes from the workspace, a fact confirmed by the corresponding increase in erosive capacity. In this case, ultrasonic activation of wire electrode ensures a productivity increase by about 59-62% higher than the W-EDM processing without ultrasonic activation (for same intensity step). Without ultrasonic activation of the wire electrode, the technological parameter is limited to an intensity step corresponding to value *3.08* A. Ultrasonic activation of wire electrode allow to continue the technological process in normal processing conditions with at least two step by intensity (4.22 A). In this case, the increase in erosion capacity is about 80-82%.

On the other hand, at the machining case with wire electrode in the ultrasonic field, the gap size shows a slight growth trend with increasing of electric current intensity. It presents stability around the value of *0.360* mm, in the range of intensities *3.08-4.22* A. Without an ultrasonic activation of the wire electrode, the cutting slit presents a minimum to a minimal current value and has a tendency to increase linearly once with the increase of intensity for the dielectric breakdown. This adversely affects the dimensional accuracy and the shape of the workpiece. Compared with the processability tests of the samples made from *34 MoCrNi15*, the average gap size is lower with approx. 0.10 mm.

Discussions:

The ultrasonic activation of wire electrode into two points after two rectangular directions in space imposes restrictions constructive nature. Thus, it is difficult and uneconomical the manufacturing and control the operation of several identical waveguides. Usually, they are designed and sized strict on the electroacoustic transducer frequency (usually piezoceramic) for as the ensemble waveguide - transducer *to operate at resonance*. At resonance, the electroacoustic yield is maxim.

Basically, the physical realization of ultrasonic transducers covers a relatively wide range of frequencies and amplitudes. From the point of view of industrial application is interesting the real case of the ultrasound efficiency on the W-EDM processing when there are functional differences between the waveguides and transducers.

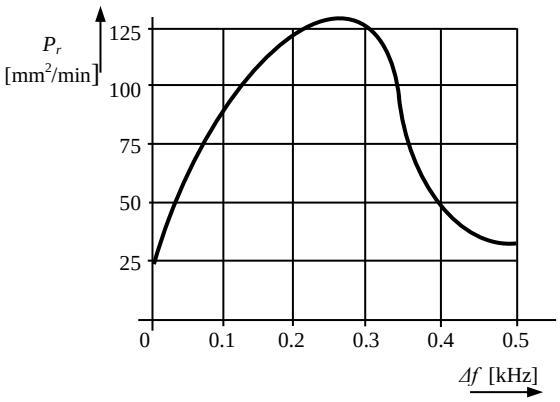

Fig. 18 Productivity of the erosion process depending on the frequency difference between the two ultrasonic activation points of the wire electrode

In Figure 18 the influence of the differences punctual frequency on the productivity of erosion process by W-EDM is described when the wire electrode is ultrasonic activated in two points after two rectangular directions in space. The range of frequency is $\Delta f = 0.26$ kHz, being between *39.90* kHz and *40.16* kHz, where 39.90 kHz is resonance frequency of guiding element in the fixed arm and 40.16 kHz is same in the mobile arm [29, 30]. Main parameters were: the movement speed of wire electrode along its axis: *25* mm/s; the stretching force of the wire electrode: *40* N; the absorbed power by ultrasonic generators: *30* W; the resistivity of the dielectric fluid: 10^4 Ω.cm; intensity for breakdown dielectric fluid: *3.50* A.

From space composition of the two oscillations resulted a component for which the difference between the working frequencies was *0.27* kHz and leaded to a maximum productivity of erosive process $P_r = 130$ mm²/min. It is noted that for values of differences less than *0.2* kHz (between primary frequencies of guide prisms of the ultrasonic activated wire electrode), is obtain a more pronounced decrease in productivity of erosive process. At values greater than *0.3* kHz erosive process productivity tends to stabilize at 30-35 mm²/min.

5.2 Dimensional accuracy and shape deviation

In order to highlight the influence of the ultrasound activation on the processing accuracy [30], we used more parts with plate shape made of same material *X210 CRW 12*, DIN 1.2436, but having *120* mm thickness. By W-EDM processing with ultrasonic wire electrode activated, were obtained punches with cylindrical shapes. The geometry of parts and the verification scheme for the workpiece accuracy after the machining process is shown in Figure 19. Samples were measured on a length measuring machine with *0.001* mm accuracy, in one operating metrological laboratory.

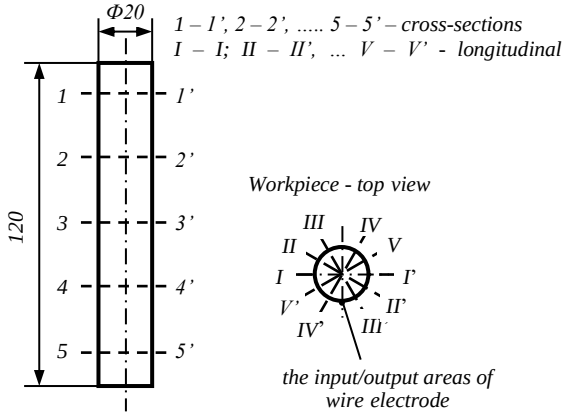

Fig. 19 Drawing and schematic diagram for dimensional accuracy and shape deviation determination after processing

Basically, the samples measurement was performed in five cross-sections named *1 - 1', 2 - 2', ... 5 - 5'*, and in each transverse plane were also performed five measurements in five points corresponding to longitudinal sections denoted *I - I', II - II', ... V - V'*. The length measuring machine was adjusted with the help of some high precision blocks with nominal dimension of 20 mm, so that:

- *deviation from the nominal dimension* is defined as being the maximum difference between the extreme dimensions measured in any of the cross-sections *1 - 1', 2 - 2', ... 5 - 5'*, respectively in any longitudinal sections *I - I', II - II '... V - V'*;

- *deviation from circularity* is defined as being the maximum difference between the extreme values measured in one of the cross-sections *1 - 1', 2 - 2', ..., 5 - 5'* after the longitudinal sections *I - I ', II - II' ... V - V'*;

- *deviation from cylindricity* is calculated by summing the maximum deviation from circularity with the maximum deviation from rectilinearity - determined as the semi-difference of extreme values measured in same cross-section *I - I ', II - II' ... V - V'* after longitudinal plans *1 - 1', 2 - 2', ... 5-5'*.

The operating data were: the movement speed of wire electrode along its axis: *55* mm/s; the stretching force of the wire electrode: *40* N; intensity for breakdown dielectric fluid: *12.68* A; the absorbed electric power by the ultrasonic generators: *30* W; resistivity of the dielectric fluid: 10^4 Ω.cm; ultrasonic activation frequency: *39.900* kHz and *40.160* kHz. Were processed by W-EDM, the workpiece having the configuration from Figure 19. Five workpieces were processed without ultrasonic activation (blank samples) and five pieces were processed with wire electrode ultrasonic activation. Test results in chronological order of processing, are summarized in *Table 3*, where US – is ultrasound.

Table 3

Dimensional accuracy of machined parts alloy steel *X210 CrW 12*, having 120 mm thickness, with and without wire electrode ultrasonic activation

Parameter [mm]		**The sample's number**				
		1	**2**	**3**	**4**	**5**
Dimensional accuracy	Without US activation	$\Phi 20^{-0.045}_{-0.110}$	$\Phi 20^{-0.066}_{-0.138}$	$\Phi 20^{-0.054}_{-0.122}$	$\Phi 20^{-0.051}_{-0.118}$	$\Phi 20^{-0.060}_{-0.128}$
	With US activation	$\Phi 20^{-0.008}_{-0.036}$	$\Phi 20^{-0.004}_{-0.031}$	$\Phi 20^{-0.010}_{-0.036}$	$\Phi 20^{-0.005}_{-0.028}$	$\Phi 20^{-0.007}_{-0.034}$
Deviation from circularity	Without US activation	*0.055*	*0.060*	*0.062*	*0.058*	*0.060*
	With US activation	*0.027*	*0.022*	*0.024*	*0.021*	*0.026*
Deviation from cylindricity	Without US activation	*0.065*	*0.072*	*0.075*	*0.069*	*0.071*
	With US activation	*0.031*	*0.028*	*0.029*	*0.027*	*0.029*

We can notice a considerable improvement in dimensional and shape accuracy at W-EDM processing with the ultrasonic activated wire electrode, compared with the processing without ultrasonic activation, which is explainable by: (1) maintaining a relative rigorously constant position of the wire electrode (which vibrates with ultrasonic frequency), relative to workpiece during the machining process, in conjunction with countering the negative influence of the electromagnetic field caused by the pulsed electrical discharges between electrodes; (2) obvious improvement to the exhaust conditions for the erosion particles from gap; (3) faster refresh of the working environment by restoring the initial dielectric fluid properties, in order to ensure the optimal conditions for disruptive breakdown.

The dispersion or the scattering field for measured parameters is significantly smaller when the wire electrode is ultrasonically activated. Thus, by measuring the processed samples - see *Table 3* - it can be observed a decrease of the scattering field from *0.093* mm (which is constantly ensured on the W-EDM machines), to *0.032* mm for workpieces processed with ultrasonically activated wire electrode, a reduction almost of three times. Moreover, the shape deviations - circularity and cylindricity - were reduced almost twice when the wire electrode was ultrasonically activated. Important is the fact that, depending on program and corrections imposed by the numerical control to an ordinary W-EDM equipment, the ultrasonic activation of the wire electrode ensures a considerable rapprochement of the probability density and tolerance field (scattering field) towards the value rated *Φ20 h7* (a common value&accuracy which for normal machine building, molds and dies, corresponds to some finished parts).

5.3 Surface roughness

To obtain low roughness for the machined surface it's necessary to work with relatively low intensity current needed for the dielectric breakdown. But low intensities of breakdown current finally lead to reduced values of erosion capacities and so, to high costs of machining. One way to improve the quality-price ratio is the ultrasonic activation of the wire electrode [30].

To highlight ultrasound influence on the quality of the machined surface, we considered a workpiece

made of *X210 CrW 12* DIN 1.2436, having a geometry and configuration illustrated in Figure 20.

The parts were treated at *60-62* HRC and have the shape of a prism in steps with heights of *10, 40, 80* and *120* mm. These were cut through W-EDM process with wire electrode, with or without ultrasonic activation, in batches of five samples for each thickness. Depending on each thickness, it was adjusted the breakdown current intensity to values that provide a maximum of erosive capacity. The operating data were: the movement speed of wire electrode along its axis: *16, 25, 40* and *55* mm/s (adjustable in steps for each workpiece thickness level); the stretching force of the wire electrode: *40* N; the absorbed power by ultrasonic generators: *30* W; the ultrasonic activation frequency: *39.900* kHz and *40.160* kHz; the resistivity of the dielectric fluid: 10^4 Ω.cm.

Findings are summarized in *Table 4*, where US - is ultrasound. Values which have been measured represent arithmetic average of five consecutive samples.

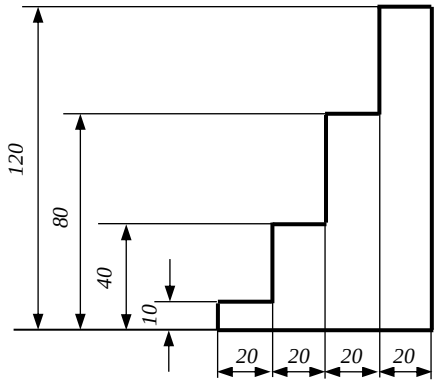

Fig. 20 Side view of a prismatic workpiece made of a high alloy steel

Table 4

Surface roughness depending on the breakdown current strength

Parameter	**Processing method**	**Intensity for breakdown dielectric fluid** I_1+I_2 [A]			
		1.88	2.74	8.74	13.88
Surface roughness of workpiece R_a [μm]	Without US activation	*1.94*	*2.35*	*3.08*	*3.62*
	With US activation	*0.81*	*0.86*	*0.96*	*1.02*

The dependence between surface roughness R_a and the working characteristics corresponding to each workpiece thickness, accounting the breakdown current intensity $I_1 + I_2$, is illustrated in Figure 21.

It is observed that in the case of ultrasonic activated wire electrode (curve **1**), there are obtained a lower roughness of workpiece surface. A statistical analysis shows that the measured values have a very small dispersion of the scattering field, between *0.8* μm and *1.0* μm, regardless the intensity value for dielectric breakdown. This phenomenon is explained by the effect of the ultrasound energy at the machining which creates smoothing of the workpiece surface. The surface obtained by W-EDM process presents micro-cavities resulting from the electrical discharges in the pulse. But this surface is additionally machined through the mechanical abrasion caused by the eroded and scattered particles into the ultrasonic field; these particles, having very high kinetic energies, they strike and smooth the workpiece surface, before being eliminated from workspace.

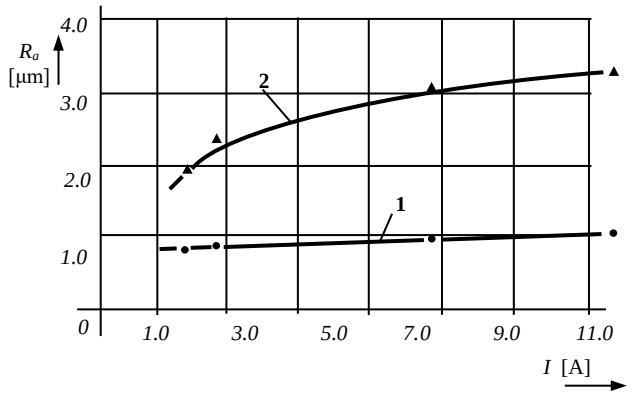

Fig. 21 Surface roughness toward variation of pulse generator intensity

It is also noted that the influence of the current intensity needed for the dielectric breakdown (*I*), respectively of the workpiece thickness, are insignificant towards the parameter R_a when the wire electrode is ultrasonic activated. When working with wire electrode without ultrasonic activation (curve **2**), the values of the surface roughness are much higher. These values are - see *Table 4* - between *2.0* μm and *3.5* μm. It is observed that there is a direct proportionate link between the values of intensity needed for the dielectric liquid breakdown (*I*), respectively the workpiece thickness, relative to the parameter R_a - more obvious at lower values for intensity.

4. CONCLUSIONS

Ultrasonic activation of the wire electrode to the nominal frequency $f = 40$ kHz, simultaneous in two points after two directions rectangular into space, has led to an increase in the W-EDM processing productivity. This increase of erosive capacity can reach, under certain conditions, even to 80-92%.

Ultrasonic activation of the wire electrode has allowed increasing the electric current intensity for breakdown dielectric liquid to values that normally, cannot be obtained only by EDM machining. In all cases studied, ultrasonic activation of the wire electrode has led to an increase of electrical current intensity for breakdown dielectric liquid by at least two steps.

On the other hand, ultrasonic energy transmitted to the wire electrode and, thus to the working environment, has ensured unfolding the electro-erosive processes to tensile forces relatively low. As such, the wire electrode has not been subjected to a mechanical stress close to the breaking limit. In this way, were avoided frequent breakages of the wire electrode; thus, was positively influenced the dimensional accuracy of workpieces.

Also, ultrasonic energy which was transmitted to the wire electrode, partially or totally has annihilated effect of the electromagnetic field generated between the electrodes due to electrical discharges in pulse. In this way, it was possible to avoid short-circuits, which have negative effects on productivity processing, dimensional accuracy and surface quality.

Some performances obtained worldwide regarding the erosive capacity of machining process by EDM with vibrational wire electrode is closely related to the construction and performance of pulse generators. Researchers such as Mițkevici [15] (which obtained increasing the erosive capacity about *2-2.5* times) and Inoue [20] (which obtained increasing the erosive capacity about *1.8-2.3* times), have achieved outstanding results for the first variants of RC pulse generators. Currently, the electro-erosive pulses generator ensures high cutting speeds without ultrasonic activation of wire electrode, frequently reaching values of *120-160* mm^2/min or even more. For this reason, increasing the erosive capacity for the current types of voltage pulse generators which equips the W-EDM machines is relatively low even if working into ultrasonic field. Only the optimal combination between the powers of the two ultrasound generators used to ultrasonic activation of the wire electrode in two points after two rectangular directions in space enabled a growth in the erosive capacity, for same current intensity level, with approx. 91-92%.

In all cases studied, the ultrasonic wire electrode activation led to a spectacular increase in dimensional and shape precision of machined parts. Through considerable reduction of the scattering field of random variables, it was possible to bring the maximum probability density near of prescribed nominal share. Thus, there was no need for an additional correction of the wire electrode trajectory.

At the same time, roughness surface of parts processed with wire electrode ultrasonic activated is comparable with that of a grinding or finishing operation. These results were not obtained in attenuation conditions of the W-EDM process operating data. On the contrary, they were obtained in conditions by maximum productivity for electrodischarge processing. Thus:

- *increases dimensional accuracy* and *the shape deviation* because wire electrode oscillates with a constant vibration amplitude for entire thickness of semifinished and has a large enough energy to annihilate effects of electromagnetic field generated by electrical discharges in pulse between electrodes; at the same time, it is ensured a constant resistivity/conductivity of dielectric liquid from technological interstitium, to whom is added the dispersion property for eroded particles that are into ultrasonic field;

- *improves roughness surface of workpiece* because eroded particles, that are into ultrasonic field, before being dispersed, act as some abrasive tools which by hammering, smoothes surface resulting with microcavities as a result of electrical discharges in pulse.

ACKNOWLEDGEMENTS

This paper was conducted with the support of SC STIMEL SA Timisoara, Romania and University Politehnica Timisoara. On this path, I wish to thank Mr. Mâțiu Andrei, general manager at SC STIMEL SA, to machines operators and persons for quality management. Also, I wish to thank distinguished Professors like Nanu Aurel, Savii Gheorghe and Iclanzan Tudor for the professional competence wherewith they guided me during the unfolding of experimental research.

REFERENCES

[1] Liu S., Hunag Y., Li Y., *A plate capacitor model of the EDM process based on the field emission theory*, International Journal of Machine Tools Manufacturing, 51(7):653-9, 2011

[2] Mironoff N.L., *Introduction in electrodischarge study*, Publishing Micro technical, Switzerland, 1970

[3] D'Urso G., Merla C., *Workpiece and electrode influence on micro-EDM drilling performance*, Precision Engineering, 38(4):903-14, 2014

[4] Mironoff N.L.,*Thermal effects of erosive pulses*, ISEM 5, Wolfsberg, 1977

[5] Nanu A., Nanu D., *Dimensional processing by electrical erosion in magnetic field,* Facla Publishing, Timisoara, 1981

[6] Wong Y., Rahman M., Lim H., Han H., Ravi N., *Investigation of Micro-EDM Material Removal Characteristics Using RC-Pulse Discharges,* Journal of Materials Processing Technology, 140 (1-3): 303-307, 2003

[7] Nichici Al., Popovici V., Nica M., Achimescu N., Popa H., Paulescu Gh., *Processing by erosion in machine building,* Facla Publishing, Timisoara, 1983

[8] Chinmaya P.M., Sahu J., Mahapatra S.S., *Thermal-structural analysis of electrical discharge machining process,* Procedia Engineering, 51, 508-513, 2013

[9] Chinmaya P.M., Siba S.M., Manas R.S., *A particle swarm approach for multi-objective optimization of electrical discharge machining process,* Journal of Intelligent Manufacturing, Online First Articles, 1-20, 12 July 2014

[10] Kitamura T., Kunieda M., *Clarification of EDM Gap Phenomena Using Transparent Electrodes,* CIRP Annals 63 (1):213-216, 2014

[11] Okada A., Uno Y., Nakazawa M., Yamauchi T., *Evaluation of spark distribution and wire vibration in wire EDM by high-speed observation,* CIRP Annals, 59 (1), 231-234, 2010

[12] Ho K.H., Newman S.T., Rahimifard S., Allen R.D., *State of the art in wire electrical discharge machining (WEDM),* International Journal of Machine Tools and Manufacturing, 44 (12), 1247-1259, 2004

[13] Jun Q., Fei Y., Jun W., Bert L., Dominiek R., *Material removal mechanism in low-energy micro-EDM process,* CIRP Annals-Manufacturing Technology, 64, 225-228, 2015

[14] Loeb L.B., Meek J.M. *The Mechanism of the Electric Sparks,* Stanford University Press, ed. 1977

[15] Miţkevici M.K., *Ob elektroerozionnom effekte na vibrinuişcih elektrodah,* Fiziceskie osnovi elektroiskrovoi obrabotki materiallov, Editura Nauka, Moscova, 1966

[16] Nani V.M., *Ultrasound influence on the erosive capacity at the electrodischarge processing with ultrasonic activated wire electrode in a single point*, Meccanica, 52, 1459–1474, DOI: 10.1007/s11012-016-0467-2, 2017

[17] Nani V.M., *Ultrasonic activation of the wire electrode on EDM processing machine*, ISBN: 978-3-659-68755-6, LAP LAMBERT Academic Publishing, Germany, 2015

[18] Ikeda M.,*The movement of a bubble in the gap depending on the single electrical discharge (first report),* Journal of The Japon of Electrical Machining Engineers, 6 (11): 12-26, 1972

[19] Murti V.S.R., Philip P.K., *An analysis of the debris in ultrasonic-assisted electrical discharge machining*, Wear 117, 241-250, 1987

[20] Inoue K., *Procédé et dispositif pour le traitement par érosion électrique avec électrode filiforme vibrant*, Brevet France, no 2 350 919/07.10.1979, 1979

[21] Savii Gh., Nani V.M., Militaru C., Muntean N., *Method and device for ultrasonic activation wire electrode*, Romanian Patent, no 102596/12.12.1988, 1988

[22] Chen Z., Huang Y., Huang H., Zhang Z., Zhang G.,*Three-dimensional characteristics analysis of the wire-tool vibration considering spatial temperature field and electromagnetic field in WEDM*, International Journal of Machine Tools&Manufacture, 92, 85-96, 2015

[23] Hayakawa S., Sasaki Y., Itoigawa F., Nakamura T., *Relationship Between Occurence of Material Removal and Bubble Expansion in Electrical Discharge Machining*, Procedia CIRP 6:174-179,

[24] Cetin S., Okada A., Uno Y., *Effect of Debris Accumulation on Machining Speed in EDM*, International Journal of Electrical Machining, 9: 9-14, 2004

[25] SC STIMEL SA Timisoara Company, Romanian, *Electrodischarge processing machine with wire electrode and numerical command by type ELEROFIL-10*, Technical Paper, 2002

[26] Nani V.M., *Activation ultrasonic methods of wire electrode used in electrodischarge processing*, Copybook for Acoustics, Romanian Academy Publishing, no 28, 41 – 44, 1992

[27] Yamada H., Mohri N., Saito N., Magara T., *Modal analysis of wire electrode vibration in wire-EDM,* International Journal of Electrical Machining, 19-24, 1997

[28] Silaş Gh., Rădoi M., Brîndeu L., Klepp M., Hegedus A., *Collection of problems for mechanical vibrations,* Technical Publishing House, Bucharest,

[29] Nani V.M., *Effect of wire electrode's ultrasonic vibration on erosive capacity to W-EDM machines*, International Journal of Advanced Manufacturing Technology, 88, 425-441, DOI: 10.1007/ s00170-016-8752-8, 2016

[30] Nani V.M., *The ultrasound effect on technological parameters for increase in performances the W-EDM machines*, International Journal of Advanced Manufacturing Technology, 88, 519-528, DOI: 10.1007/ s00170-016-8783-1, 2016